DIAMOND-BASED SEMICONDUCTING DEVICES

Diamond is a naturally occurring crystalline form of carbon. Presence of small amounts of substitutional B in natural diamond crystals contributes to *p*-type semiconductor properties. In addition to having the highest values of thermal conductivity and hardness, diamond also has a number of unique electronic material attributes. These are its wide bandgap, predicted high carrier mobility, electron saturated velocity, breakdown field, and low dielectric constant. These properties make diamond an almost ideal material for the fabrication of devices, which can be operated at high temperatures, voltages, power levels, and frequencies, and in high-radiation environments. For the purpose of comparison, some of these parameters for the conventional semiconducting materials, such as Si and GaAs, are included in Table 1 along with those for new materials—namely, SiC and diamond. Some of the commonly used figures of merit are also included in Table 1. These figures of merit are discussed in the following sections. Some diamond surfaces also exhibit negative electron affinity (NEA), a property that is potentially suitable for the fabrication of cold cathodes for various vacuum electron devices used in displays and microwave amplifiers.

The potential of diamond as a material for solid state devices has been the subject of several excellent reviews (1–5). These reviews discuss the electronic material parameters of diamond and the simulated characteristics that can be obtained. Early efforts in device research were mainly based on prohibitively expensive, naturally occurring *p*-type diamond crystals or *p*-type homoepitaxial films deposited on insulating diamond crystals. However, processing of diamond for achieving device structures is not well established. In particular, the absence of truly heteroepitaxial films and suitable *n*-type dopants will hinder widespread device development research that attempts to realize the benefits of the predicted superlative electronic properties of diamond. Recent developments in the growth of thin films of diamond on inexpensive, nondiamond substrates have permitted the fabrication of a number of experimental devices in an attempt to realize the potential of diamond as an electronic material. In the absence of truly heteroepitaxial films of diamond, most of these studies have been conducted on polycrystalline or coalesced aligned grain films. Figure 1 shows the scanning electron micrographs of polycrystalline, highly oriented (100) textured and homoepitaxial diamond films.

Demonstrated devices include photodetectors, light emitting diodes, nuclear radiation detectors, thermistors, varistors, and negative resistance devices reported primarily by researchers in the former Soviet Union. Bipolar and basic field effect transistors have also been demonstrated by a number of research groups. Cold electron emission has been reported along with a number of advanced field effect device structures, microwave amplifier devices, and display devices, that will take advantage of the unique properties of diamond, have been proposed.

In this review, first we consider the various figures of merit that can be used for assessing device performance on a given material in order to determine the potential of diamond as an electronic material. In subsequent sections, we consider various process steps involved in the fabrication of diamond devices. Generally, these steps include controlled doping of films, as well as selected area doping, etching, formation of ohmic and rectifying contacts, either deposition or formation of dielectric films, and passivation of the surface. Finally, demonstrated device structures and their performance are discussed, including the current status of diamond cold cathode devices.

FIGURES OF MERIT

A figure of merit (FOM) can provide a basis derived from physical theory for comparison of device potential among different semiconductors. The Keys FOM (6) is an indication of the thermal limitation of a material on its high frequency performance. The Johnson FOM (7) relates to the frequency and power product of a semiconductor device. The Keys and the Johnson FOM relate to materials for use in transistors for high speed electronics and millimeter wave applications. Baliga (8) derived the BFOM, which applies to systems operating at low frequencies where the conduction losses are dominant. He also derived the BHFFOM, which is used to evaluate the high-frequency switching capability of devices. Shenai et al. (2) have also developed a set of FOM using the peak electric field strength at avalanche breakdown as the critical material parameter. The FOM introduced by Baliga and Shenai et al. are considered to be appropriate for the evaluation of semiconductor materials for power device applications. More recently, Chow et al. (9) have calculated the above mentioned FOM for a number of semiconductors taking into account the nonlinear power relationship between the energy bandgap

J. Webster (ed.), *Wiley Encyclopedia of Electrical and Electronics Engineering*.

Table 1. Comparison of Important Properties of Selected Semiconductors

Property	Si	GaAs	α-SiC	β-SiC	Diamond
Band Gap (eV)	1.1	1.4	2.9	2.3	5.5
Therm. Cond. (W/cm · K)	1.5	0.46	4–5	4–5	20
Phase Change (°C)	1415	1238	sublime $>$1800	sublime $>$1800	$>$1200
Mobility (cm^2/V · s)					
Electron	1400	8500	400	800	2200
Hole	600	400	40	70	1600
Sat. Electron Vel. ($\times$ 10^7 cm/s)	1.0	1–2	2.0	2.5	2.7
Breakdown ($\times$ 10^5 V/cm)	3.0	4.0	10–50	10–50	10–200
Dielectric Constant	11.8	12.5	10	9.7	5.5
Johnson FOM*	1.0	11	260	110	6220
Keys FOM*	1.0	0.45	5.1	5.8	32
Baliga FOM*	1.0	28	90	40	11700
Baliga HFFOM*	1.0	16	13	12	850
QF1*	1.0	9.4	300	130	155990
QF2*	1.0	16	2440	550	4554840
QF3*	1.0	28	90	40	11700

[a] Data from Chow et al. (9).

and critical electric field. Table 1 includes the FOM for the selected semiconductors. It is clear that wide bandgap materials have superior electronic attributes and that diamond appears to be well suited for high speed and high power devices.

DEVICE PROCESSING

Doping

The incorporation and activation of dopants reproducibly and controllably, as well as the understanding and characterization of the associated physical processes of compensation, carrier transport properties, and the presence and activity of deep-level states are of fundamental importance for an emerging device technology.

Boron has been identified as the dopant responsible for *p*-type behavior in naturally occurring semiconducting diamond (10). From geometric and energetic considerations, B is probably the only element that can substitutionally dope diamond without generally distorting the lattice. The activation energy associated with B in diamond is 0.37 eV (10,11). Boron has been incorporated into homoepitaxial and polycrystalline films during chemical vapor deposition (CVD) from either a B_2H_6 gas source or from various solid sources (12–14). For relatively small concentrations, the activation energy is close to the characteristic 0.37 eV. For highly doped (10^{19}–10^{20} cm^{-3}) films, almost total activation is achieved (12–14), and activation energies as low as 0.002 eV have been reported.

In addition to in situ doping of the CVD grown films, ion implantation offers an alternative technique for the introduction of electrically active impurities in a more precisely controlled manner. Experiments conducted by Vavilov et al. (15), Braunstein and Kalish (16), and Prins (17) have shown promising results. These early studies have been recently reviewed by Prins (18), Kalish (19), and Das (20). Extensive radiation damage occurs in diamond implanted with a B dose exceeding $\sim 1 \times 10^{15}$ cm^{-2}. This damage leads to the formation of a surface layer of graphite upon annealing. Braunstein and Kalish

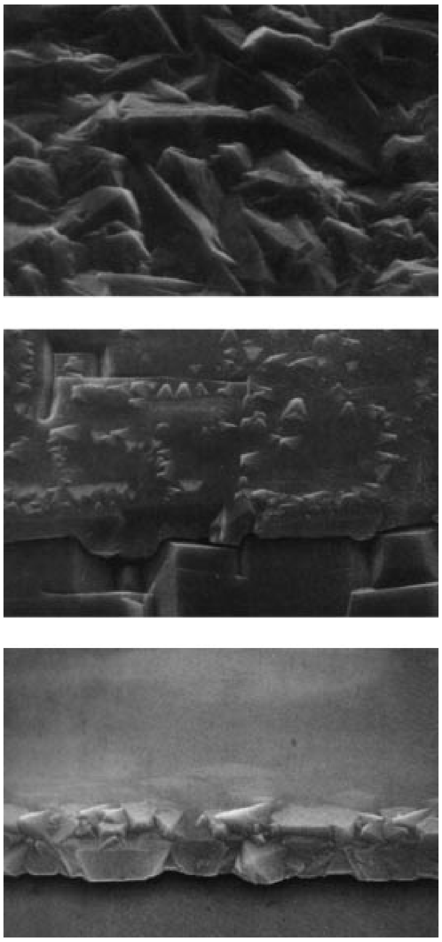

Figure 1. Scanning electron micrographs of polycrystalline (3 cm = 10 μm), highly oriented (100) textured (3 cm = 10 μm) and homoepitaxial (5 cm = 10 μm) diamond films. Reprinted with permission from Kobe Steel USA Inc., Electronic Materials Center, RTP, NC 27709.

in their implantation doping experiments used a B dose of $\sim 1 \times 10^{16}$ cm^{-2} at 40 keV. The resulting layer of graphite was removed by chemical etching. A portion of the implanted B distribution was retained in the substrate. This remaining distribution of B was sufficient to provide a highly conducting surface layer suitable for establishing ohmic contacts. Hall mobility of this layer was determined to be 0.5 cm^2/Vs. Another approach used by Prins (18) was to coimplant B and C at liquid N_2 temperature with a subsequent high temperature anneal treatment. The implantation of C introduced vacancies at a depth that overlapped with the profile of subsequently implanted B. Thus, the probability of substitutional incorporation of B through vacancy-interstitial recombination during subsequent annealing was enhanced. Both rapid thermal annealing directly from the liquid N_2 implant temperature and furnace annealing was employed. Prins subsequently reported that the donor activity associated with implant damage cannot be completely removed by thermal annealing treatment at temperatures below 1650°C.

Relatively high Hall mobilities have been observed in B doped diamond films. Using Hall-effect measurements, the transport properties of different diamond films have been measured. The room temperature mobilities of 1590 cm^2/Vs, 229 cm^2/Vs and 70 cm^2/Vs have been measured for the homoepitaxial, highly oriented, and polycrystalline CVD diamond films (21). It is believed that the alignment of the grains improves the transport properties of the oriented grain diamond films. In comparison, typical mobilities in natural type IIb diamond range from 500 to 1000 cm^2/Vs; the highest ever reported value being 2000 cm^2/Vs (22).

For flexibility in device design and operation, it is of great advantage to be able to introduce shallow *n*-type dopants in diamond; however, *n*-type electrical activity has not been observed in natural or synthetic crystals. Nitrogen, a commonly occurring impurity in natural diamond, is a deep donor with an energy level of 1.7 eV below the conduction band-edge (10). This level is electrically inactive, although it acts as a recombination center (10). Numerous efforts to dope diamond *n*-type by implanting various ions, such as Li, P, As, Sb, C, Kr, and Xe have been reported (23). In some cases, observed *n*-type activity was attributed to residual damage. Following annealing at high temperatures, the *n*-type behavior was not retained in these samples (15). Incorporation of Li and P during CVD growth of diamond films has also been attempted for *n*-type doping (24–26). One such study indicated that in-situ Li incorporated during CVD film growth were electrically neutral; however, at high concentrations, Li appeared to degrade the measured Hall mobility (24). Recent reports by Prins (27) and Popovici et al. (28) indicate promising results. Prins obtained *n*-type conductivity by implanting a small dose of P at liquid nitrogen temperature and subsequent activation of the dopant by a rapid high temperature anneal. Popovici et al. obtained *n*-type doping by bias enhanced diffusion of Li and O_2. However, more research is required in this area in order to establish reproducible *n*-type doping procedures that could be used both for device fabrication and to confirm that any *n*-type behavior observed is due to dopant incorporation, not lattice distortion or damage.

Etching

Reproducible and controllable etching of diamond has been demonstrated by Beetz and Lincoln using an electron cyclotron resonance (ECR) plasma technique (29). The substrates were immersed directly into the plasma, and reactants such as O_2 and NO_2 were employed. Line features as small as 0.3 μm were delineated using a thin mask of deposited Au. An etch-rate of several hundreds of Å/min was achieved. Efremow et al. (30) reported successfully dry etching of diamond using a 2 keV Xe^+ ion beam and a directed flux of NO_2 molecules. Kobashi et al. (31) reported an electron-beam assisted technique employing a self-focused, intense electron beam with enclosed plasma. These researchers employed a mixture of H_2, O_2, and He.

Contact Formation

Most, if not all, solid state devices require ohmic and rectifying contacts for their operation. Formation of these contacts constitute some of the critical process steps. In the following sections, we review and discuss the formation of ohmic and rectifying contacts to diamond and factors affecting these contacts. Processes as have been employed by various researchers in their attempts to fabricate contacts on diamond, both polycrystalline films and single crystal substrates, are also reviewed.

Chemical vapor deposited diamond films contain a considerable amount of H since the deposition is conducted in an H plasma environment. Electrical effects of H and associated active-defects arising from complex interaction between H, plasma induced defects, and grain boundaries can significantly influence contact properties. Acceptor states associated with intentionally introduced B during CVD growth also interact with hydrogen-induced and other defects present in the film.

The (001) surfaces of as-deposited homoepitaxial CVD diamond films exhibit 2 × 1 reconstructed surfaces, and the unit of the reconstruction is a carbon dimer (32). Using molecular orbital calculations, it was determined that each dangling bond of a dimer is terminated by one hydrogen atom. Scanning tunneling microscopy revealed the surfaces to be totally composed of a hydrogen-terminated structure. High quality Schottky diodes with ideality factors close to unity (1.01, 1.04, and 1.13 for Al, Pb, and Zn point contacts, respectively) have been fabricated on the (001) 2 × 1 surfaces. The ideality factors for Pb and Al dot contacts averaged 1.32 and 1.33, respectively. The Schottky barrier heights depend on the electronegativity of the metal (32). In general, metals with low electronegativities exhibited good Schottky characteristics, while those with high electronegativities (like Au, Pt) exhibited ohmic characteristics. Thus, the surface states, which cause Fermi level pinning, are effectively reduced by the hydrogen-terminated (001) 2 × 1 surfaces (32).

It is also well known that the presence of H significantly modifies the resistivity of diamond films. As-deposited undoped films exhibit fairly low resistivities of the order of 1×10^6 Ωcm. Annealing of these films at temperatures as low as 400°C increases the resistivity by a few orders of magnitude. The observed increase in resistivity has been attributed to a partial dehydrogenation (33) of the films resulting in the activation of deep traps with a consequent increase in resistivity (34,35).

The presence of a low resistivity, nondiamond surface-layer in as-grown films has also been inferred from current-voltage (I–V) measurements on metal contacts (Au) to homoepitaxial diamond films (36). However, these layers were successfully removed by treating in a boiling solution of CrO_3 in concentrated H_2SO_4. Subsequent to further cleaning in boiling H_2O_2 and NH_4OH, these films with deposited Au dots produced high quality rectifying contacts. Similar results have also been reported by Mori et al. (37) in their investigation of CVD diamond films. According to Mori et al., surface treatment of diamond films in a hot solution of CrO_3 in H_2SO_4 or in an O plasma results in a submonolayer oxygen coverage of these films. They concluded that contact characteristics on CVD diamond films without O on the surface depend on the electronegativity of the metal, while those on films with O on the surface do not exhibit such a dependence. From a Kelvin probe and X-ray photoelectron spectroscopy (XPS) study of contact potentials, Shirafuji et al. (38) concluded that the energy band of the as-grown surface bends upward to form an accumulation layer for holes owing to the existence of acceptor-type surface states well below the bulk Fermi level. However, on O terminated surfaces produced by O_2 ambient annealing or O plasma treatment (also chromic acid treatment), there is a depletion layer for holes due to the existence of donor-type surface states existing ~1.7 eV above the valence band. The origin of these surface states were not established.

A stabilization anneal and a thorough cleaning to remove any nondiamond component from the surface is important for obtaining a starting material with a reproducible surface preparation for device processing. Preferred cleaning procedure involves treatment in boiling solution of CrO_3 in H_2SO_4 treatment followed by an RCA (39) cleaning procedure, although this procedure contributes to a submonolayer coverage of the surface with O.

Electrical contacts with desirable ohmic or rectifying characteristics cannot normally be established on annealed films without further surface treatment. Undoped or nominally B doped films with metal contacts normally yield an "S" shape I–V curve. Ohmic contacts can, however, be established with any conducting material (metals, silicides, carbides, or highly doped semiconductors) on highly B doped films. Surface treatment procedures for establishing rectifying contacts normally include the deposition of a thin passivating surface layer of undoped diamond or a thin film of deposited SiO_2. In the case of deposited SiO_2, rectifying contacts are observed for films of tunneling thickness ~30 Å. For thicker deposited SiO_2 films, MOS type characteristics are observed. Contacts established with thin undoped diamond as passivating films on doped diamond films are more robust in device applications.

For achieving ohmic contacts, a highly doped surface layer deposited by either CVD (4) or ion implantation of B is normally employed (18–20). Sputter deposition (Au) induced surface damage also contributes to an ohmic contact. However, using evaporated Au dots, Grot et al. (36) observed ohmic-like behavior on as-deposited homoepitaxial film.

In the case of naturally occurring B doped semiconducting diamond type IIb with a cleaning treatment involving oxidizing chemicals, namely, boiling solution of CrO_3 in H_2SO_4 and RCA cleaning solutions, rectifying contacts are formed with any metal or conducting system, such as refractory silicides and carbides and highly doped amorphous or polycrystalline Si. In the case of both IIb and insulating crystals with a highly B doped surface, any of the above-mentioned conducting systems contribute to ohmic contacts.

Ohmic Contacts. For the operation of most solid state electronic devices, it is essential to form a low resistance ohmic contact. A number of researchers have studied the formation of ohmic contacts primarily to natural IIb crystals. A small number of reports also involve ohmic contacts to polycrystalline films. Table 2 summarizes the major findings reported. An excellent review by Moazed et al. (42) describes earlier work in the area of ohmic contact formation, including recent results obtained using carbide forming refractory and transition metals protected by an overcoat film of Au.

In recent device studies or for electrical characterization single crystal and polycrystalline films, generally a thin film of a refractory carbide forming metal of 100 to 500 Å in thickness is sputter deposited, followed by an overcoat film of Au 1000 to 1500 Å in thickness by sputtering or e-beam evaporation. A subsequent anneal at 800 to 900°C is employed to form a carbide at the interface between the diamond and the refractory metal film. The formed carbide establishes the ohmic

Table 2. Ohmic Contacts to Diamond

Metallization	Annealing condition	Diamond surface	ρ_c at RT (Ω cm^2)	Reference
Ag		Damged		Prins (40)
W				Geis et al. (41)
Metal carbides: Au/Ta, Au/Ti, Au/Mo	885°C/8–16′			Moazed et al. (42) Tachibana et al. (43,44)
Si/SiC	1200°C/60′	Kr' damaged	1×10^{-3}	Fang et al. (45)
Au		Ar^+ damaged		Childs et al. (46) Tachibana et al. (44)
W probe		High dose B I/I, anneal and graphite removal		Sandhu (47) Prins (48)
Metal carbide: Au/Ti		In-situ B doped (~10^{20} cm^{-3})	2×10^{-5}	Hewett et al. (49)
Metal carbide: Au/Ti	850°C/30′	High dose B I/I, anneal and graphite removal	1×10^{-5}	Venkatesan et al. (50)
Metal carbide: Al-Si(99:1)	450°C	In-situ B doped (~8×10^{21} cm^{-3})	2×10^{-7}	Werner et al. (51)

contact. A specific contact resistance of 2×10^{-5} Ωcm^2 was reported by Hewett et al. (49) obtained from a contacts established on homoeopitaxial films with a doping concentration $\sim 1 \times 10^{20}$ cm^{-3}. Several research groups have employed a high-dose B implantation step to produce a high B concentration surface layer on the diamond to produce contacts with low specific contact resistance. High-dose ion implantation introduces an extensive radiation damage leading to graphitization of the surface layer during a subsequent anneal treatment at 1200°C in a vacuum. The graphitized surface is removed by boiling in a solution of $HClO_3 + HNO_3 + H_2SO_4$ (1 : 4 : 3) or CrO_3 in H_2SO_4. With a surface concentration of $1 \times 10^{20} - 1 \times 10^{21}$ cm^{-3}, an ohmic contact can be achieved with any deposited metal or probe contacts. However, a further annealing with a Ti/Au bilayer film yields specific resistance of the order of 1×10^{-5} Ωcm^2. It has further been demonstrated that for a sputter deposited TiC film from a preformed target overcoated with a film of Au on highly doped diamond substrates, a specific contact resistance of the order of $\sim 1 \times 10^{-5}$ Ωcm^2 can be obtained without a contact forming anneal step. Annealing of these contacts did not improve or degrade the as-deposited contact resistance (52).

Rectifying Contacts. In general for a *p*-type semiconductor, if the semiconductor work function is greater than the metal work function, the metal forms a rectifying contact on the semiconductor. Work-function differences between diamond substrates [both (100)- and (111)-orientations] and Al electrodes have been determined by performing *C–V* measurements on metal-SiO_2-diamond structures (53). This structure also enabled the determination of the electron affinities of (100)- and (111)-oriented diamond substrates. Accordingly, electron affinities of 2.3 eV and −0.7 eV have been reported for the (100)- and (111)-oriented substrates, respectively (53). Thus, based on this finding by Geis et al. (53), it could be inferred that any metal should form a rectifying contact on the (100)-oriented substrate.

Rectifying contacts to natural (54) and synthetic high-pressure-high-temperature grown diamond crystals (11) have been reported. Rectifying contacts established on homoepitaxial and polycrystalline films also have been reported. Various metals, silicides, carbides, highly-doped polycrystalline, and amorphous Si have been employed as the contact material. Table 3 summarizes the reported results. The general observation is that rectifying contacts on IIb diamond crystals are readily established with any conducting material system including elemental metals, highly doped semiconductors, silicides, and carbides. These rectifying diodes show very low reverse leakage currents up to hundreds of volts. In most cases, avalanche breakdown is not observed due to edge leakage,

Table 3. Rectifying Contacts to Diamond

Metallization	Diamond surface	Rectification (*I–V*)	ϕ_B (eV)	ϕ_B meas technique	Reference
All metals	(100)				Geis et al. (53)
Metal/insul diamond/semi diamond	homoepi/ polycryst	∼nA leakage at 20 V reverse			Shenai et al. (55) Miyata et al. (56)
Metal/∼20 Å SiO2/semi diamond	homoepi/ polycryst	∼nA leakage at 7 V reverse			Venkatesan et al. (57)
Metal	F^+, B^+, C^+ I/I surface				Das et al. (58)
Heteroepi Ni	type IIb (100)	∼nA leakage at 20 V reverse up to 400°C			Humphreys et al. (59)
Heteroepi Cu	type IIb (100)	∼nA leakage at 20 V reverse up to 400°C	1.1	UPS	Humphreys et al. (60)
$TaSi_2$	type IIb (100)	∼nA leakage at 20 V reverse up to 400°C			Sahaida et al. (61)
P doped Si	type IIb (100)	∼nA leakage at 20 V reverse up to 400°C			Venkatesan et al. (62)
Au	(100), chem cleaned		1.7	*C–V*	Glover (11)
Au	chem cleaned		1.7–2	*C–V,* IPS	Mead et al. (63)
Au	chem cleaned		1.9–2	*C–V,* IPS	Mead et al. (63)
Pt, Au, Al P doped Si	type IIb, (100) chem cleaned		2.3	*C–V*	Venkatesan et al. (64)
Au	typeIIb, (111) (1 × 1)		1.3	ES w/synch radiation	Himpsel et al. (65)
Al	typeIIb, (111) (1 × 1)		1.5	ES w/synch radiation	Himpsel et al. (65)
Al, Au	polycryst		1.13	IPS	Hicks et al. (66)
Au	polycryst		2/1.2	IPS	Beetz Jr. et al. (26)

which results in a soft breakdown at relatively high voltages. In most cases, sharp forward turn-on is observed. These devices retain their diodelike characteristics at temperatures as high as 580°C (36) with relatively small increase in the reverse leakage current. Relatively high barrier heights restrict the forward current in the micro to nanoampere range. Contacts established with Au, heteroepitaxial Ni, and polycrystalline Si with high P doping appear to be very stable at elevated temperatures and do not show any degradation with temperature cycling. However, adhesion of evaporated metal films to highly polished crystalline diamond is poor. Titanium silicide contacts, either sputter deposited from a preformed target or coevaporated films of Ti and Si to form stoichiometric $TiSi_2$ upon anneal, also provide good rectifying contacts. Reported barrier heights for these contacts range between 0.8 and 2.4 eV. These measurements were obtained using various techniques, such as capacitance-voltage (C–V), internal photoemission, X-ray photoelectron spectroscopy (XPS), and ultraviolet photoelectron spectroscopy (UPS). Since sample cleaning techniques and surface preparation between various laboratories vary widely, individual observations cannot be compared directly. However, in one systematic study, for a given surface preparation using oxidizing wet chemicals (namely, boiling solution of CrO_3 in H_2SO_4, hot aqua regia treatment, followed by RCA cleaning procedure) and in the absence of a surface reaction, barrier heights were observed to be constant at approximately 2.3 eV regardless of the metal work function (metals employed in this study were Al, Ni, Au, Pt). However, using an approach originally developed for adjusting Schottky barriers for metal contacts to Si (67), these barrier heights for diamond rectifying contacts can be adjusted by employing a low-energy, low-dose ion-implantation step. The implantation step introduces additional ionized donors or acceptors within the space-charge layer arising from the contact potential. This additional charge modifies the surface electric field which, in turn, will modify the image force component that influences the barrier height. For acceptor implant in a p-type substrate, a reduction in the effective barrier was observed, whereas introduction of donors contributed to an increased barrier height. In the reported study on barrier adjustment for Au contacts to diamond, the donor was contributed by partially annealed stable damage introduced by a low-dose implantation of B ions (68). Diodes that had a reduced barrier height obtained with B acceptor implantation (B concentration, in this case, was greater than the residual damage contributed donors) showed a lower turn-on voltage and a higher reverse leakage in comparison with untreated contacts. The reduced barrier contacts also conducted a higher forward current.

With CVD grown films both homoepitaxial and polycrystalline, rectifying contacts cannot normally be established with directly deposited conducting films. Surface treatment procedures for establishing rectifying contacts on these CVD films normally include the deposition of a thin passivating surface layer of undoped diamond (55,56) or a thin film of deposited SiO_2 (57) prior to metallization. In case of deposited SiO_2, rectifying contacts are observed for films of tunneling thickness $\sim$30 Å (for thicker deposited SiO_2 films, MOS type characteristics are observed). Contacts established with thin undoped diamond as a passivating film on doped diamond films are more robust in device applications. Rectifying contacts on polycrystalline films has also been improved by introducing a low concentration of donors contributed by partially annealed implantation damage (20).

MOS Capacitors

A study of metal-SiO_2-semiconducting diamond (MOS) structures were first reported by Geis et al. (53). By performing C–V measurements on the MOS structures, Geis et al. determined the work-function differences between diamond substrates [both (100)- and (111)-orientations] and Al electrodes. This, in turn, enabled the determination of the electron affinities of (100)- and (111)-oriented diamond substrates. Accordingly, electron affinities of 2.3 and -0.7 were reported for the (100)- and (111)-oriented substrates, respectively. More recently, a comparative study of metal-semiconducting (MS), metal-insulating diamond-semiconducting diamond (MIS), and metal-SiO_2-semiconducting diamond (MOS) electrical contacts on natural type IIb single crystals has been conducted (69). The measured impurity concentrations ($\sim 2 \times 10^{13}$ cm^{-3}) determined by C–V technique were in good agreement with the atomic boron concentration values determined by SIMS. The density of interface states was estimated to be $\sim 10^{12}$ cm^{-2} eV^{-1} for these structures (69). The MIS contacts had a reverse leakage current two orders of magnitude lower than that of MS contacts. The turn-on voltage of the MIS contacts was $\sim$1.75 V, while that of the MS contacts was $\sim$0.5 V. The capacitance-voltage measurements on the MS and MIS contacts exhibited little frequency dependence (69).

THREE-TERMINAL DEVICES

The inability to reproducibly achieve n-type doping of diamond has limited the number of three-terminal devices that could be fabricated on diamond. Most three-terminal devices fabricated so far have been restricted to field-effect transistors (FETs). Due to surface related problems, all the FET devices reported to date (3,24,49,55,70–75), with the exception of one (76), use an insulator or a dielectric film between the metal gate and the channel region. Figure 2 shows a schematic of a diamond FET with SiO_2 or intrinsic diamond as the insulator. The best reported transconductance is only 1.3 mS/mm, one order of magnitude less than those of 3H–SiC metal-semiconductor (MES) FETs. Recently, Shin et al. (5) have studied diamond MESFETs in comparison with 6H–SiC MESFETs by two dimensional device simulation and concluded that the drain current and the operation frequency are restricted by the deep acceptor level of boron, 0.37 eV in diamond.

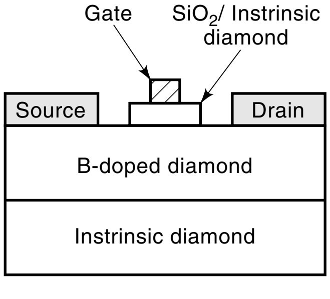

Figure 2. Schematic of a diamond field effect transistor formed with SiO_2 or intrinsic diamond as the gate insulator.

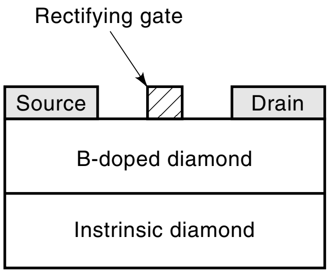

Figure 3. Schematic of a diamond metal–semiconductor field effect transistor.

Prins (40) reported the fabrication of a bipolar transistor on a *p*-type semiconducting natural crystal substrate. The *n*-type regions of the device were fabricated via carbon implantation, which produced a radiation damage induced doping effect. In spite of the low current gain, the device demonstrated the first bipolar transistor action in diamond. A point contact diamond transistor was fabricated by Geis et al. (41). The device was fabricated on a synthetic B doped diamond crystal and demonstrated a transistor action up to ~510°C. Geis et al. (77) also reported a vertical channel FET fabricated on a natural semiconducting substrate. A transconductance of 30 μS/mm was calculated from the transistor characteristics. Gildenblat et al. (3) fabricated an FET on a homoepitaxial film deposited on an insulating natural (type Ia) crystal. A sputter deposited SiO_2 formed the gate dielectric. This device showed transistor action up to 300°C. Grot et al. (74) have fabricated an insulated gate field-effect transistor with a recessed gate. The device was fabricated on B doped homoepitaxial films deposited on natural (type I a) diamond crystals. The devices were operational at temperatures up to 350°C with a maximum measured transconductance of 87 μS/mm.

Shiomi et al. (55) reported the first metal semiconductor field-effect transistor (MESFET) based on diamond. The substrate was a type Ib natural crystal on which initially, an undoped diamond film and then a B doped diamond film were deposited by a microwave plasma enhanced CVD (MPECVD) process. Aluminum formed the gate contact, while Ti formed the ohmic source and drain contacts. The device showed a transconductance of 2.0 μS/mm. Figure 3 shows a schematic of a diamond MESFET. A diamond *p*-type depletion mode MESFET was fabricated by Tsai et al. (76). The device was fabricated on a type II a insulating diamond crystal. The active channel region was formed by solid-state diffusion of B from a cubic BN source by rapid thermal processing (RTP). While as deposited Ti/Au formed the gate contacts, annealed Ti/Au formed ohmic source and drain contacts. The device was observed to pinch off at a high positive gate bias, and a transconductance of 0.7 μS/mm was obtained. Kawarada et al. (78) have reported enhancement-mode MESFETs on homoepitaxial B doped diamond films. The devices were fabricated on hydrogenated diamond surfaces which exhibit surface conduction. This surface is usually removed by etching in acids. However in this work, this layer was employed to fabricate enhancement-mode devices that exhibit saturation and pinch-off. A maximum transconductance of 200 μS/mm was obtained at room temperature.

An insulated gate field-effect transistor was fabricated by Fountain et al. (24) using selectively grown B doped homoepitaxial films on type Ia natural crystals. The SiO_2 film, which formed the gate dielectric, was deposited using a remote plasma enhanced CVD process. The source, drain, and gate contacts were formed using Ti. The device showed a transconductance of 38 μS/mm. Hewett et al. (49) reported the fabrication of metal insulator gate field effect transistor (MISFET) with an implantation doped active layer in a type IIa substrate. Here again, SiO_2 was used as the gate dielectric. A bilayer Mo/Au metallization was used as the source and drain contacts, while Ti/Au formed the gate contact. This device showed current saturation and pinch-off. Also, a transconductance of 3.9 μS/mm was obtained. Subsequently, better characteristics were obtained for a similar device fabricated on a natural type IIa diamond sample (72). A trilevel B− implant procedure was used to form the channel of the device. Source and drain contacts were formed using Mo/Au, while Ti/Au was used for gate metallization. Ohmic contacts were formed using Ti/Au as well as Mo/Au metallization and characterized using a circular TLM pattern. Contact resistances of the order of ~10^{-5} and 10^{-3} Ωcm^2 were measured and are considered to be satisfactory for device fabrication. The devices exhibited saturation and pinch-off characteristics. A transconductance of 28 μS/mm was measured at room temperature. A simple source-follower circuit was fabricated, and a voltage gain of 2 was measured at room temperature. This lower than expected gain is attributed to mechanical damage to the gate oxide resulting from the contacting probes. Recently, depletion-mode metal-SiO_2-diamond FETs fabricated on homoepitaxial diamond films exhibited saturation and pinch-off at temperatures as high as 773 K (72). The active channel was formed by in-situ B doping during CVD of diamond films. The FETS were fabricated in a concentric ring structure in order to isolate the source and drain ohmic contacts. The major advantage of this geometry is that the active device area delineation or mesa formation is not required as the current flows radially within the device. The gate dielectric was SiO_2, ~750 Å in thickness. While Au was used as the gate metal, a bilayer Ti/Au formed the ohmic source and drain contacts. The highest normalized transconductance measured was 1.3 μS/mm and source-to-drain currents of 9.7 mA. Devices were biased in a common source amplifier configuration, and voltage gains of 1.4 and 4.8 were measured at 350 K and 523 K, respectively (72). The gain versus frequency data exhibited roll-off characteristics of a circuit dominated by a resistance-capacitance time constant. Digital logic circuits were fabricated by combining two diamond FETs into NAND and NOR circuits (79). Successful operation of these simple circuits at 373 K has been demonstrated.

Junction field effect transistors have been fabricated on homoepitaxial diamond films by Plano et al. (75). These films were doped with B for the channel and P for the gate junction diode. The P doped region did not exhibit an *n*-type behavior but was equivalent to an undoped region. Some modulation with a maximum room temperature transconductance of 10 μS/mm and channel current of 1.3 mA was reported.

The first demonstration of field-effect transistors on polycrystalline diamond films was reported by Tessmer et al. (80). Ion implantation was employed to form a B-doped conducting surface channel. A low temperature deposited SiO_2 was used as the gate dielectric. While Al was used as the gate metal, Au formed the ohmic source and drain contacts. Although the channel did not pinch-off, a large modulation of the channel conductance was observed with an estimated transconductance of 121 μS/mm. Subsequently, Tessmer et al. (71) and Dreifus et al. (81) have fabricated polycrystalline diamond FETs, which show saturation and pinch-off characteristics. However, complete pinch-off of the channel current was not possible above room temperature. A parasitic leakage path through the underlying Si substrate was suspected. The active channel was formed by in-situ B doping during CVD of diamond films. The gate dielectric was SiO_2, ∼750 Å in thickness. While Au was used as the gate metal, a bilayer Ti/Au formed the ohmic source and drain contacts. At 150°C, the devices exhibited saturation of the drain current and a peak transconductance of 35 nS/mm. These devices operated at temperatures up to 285°C and drain-to-source voltages of up to 100 V. A maximum transconductance of 0.3 μS/mm was obtained at 250°C. Above 285°C, high gate leakage currents resulted in poor device characteristics. The devices fabricated on randomly oriented polycrystalline diamond substrates were compared with those fabricated on (100) highly-oriented and single crystal diamond insulating substrates (81). The transistors fabricated using highly oriented diamond films exhibited a maximum transconductance of 100 μS/mm. These transistors were characterized to a temperature of 400°C before gate failure occurred. Devices fabricated from single crystal diamond were tested up to 550°C before current leakage prevented proper device operation. For the case of the single crystal and highly oriented polycrystalline diamond devices, both saturation and pinch-off of the channel current were observed at elevated temperatures. Field effect transistors fabricated on diamond films grown on substrates other than Si have also been reported. Recently, Nishimura et al. (82) reported MISFETs on polycrystalline diamond films grown on Si_3N_4 substrates. The depletion-mode devices showed current saturation and pinch-off up to 300°C. A transconductance of 0.23 μS/mm was observed at 300°C. Device operation up to 400°C was achieved.

Devices base on pulse-doped or δ-doped diamond films have also been investigated (83–85). This method was proposed to improve the activation efficiency for the B impurity in diamond (83). According to Kobayashi et al. (83), in pulse-doped films efficient excitation of the holes from the deep level is possible because the Fermi-level approaches the acceptor level. Also, most of the excited holes are in the surrounding unintentionally doped diamond spacer layers, where holes can move with high mobilities. Shiomi et al. (84) fabricated MESFET devices using a single pulse-doped layer. This single, heavily doped layer was ∼200 Å in thickness with a maximum atomic B concentration of 1×10^{19} cm^{-3}. Modulation of the channel current, saturation, and pinch-off were observed. A maximum transconductance of 388 μS/mm was reported. Recently, Vescan et al. (85) have fabricated pulse-doped MESFETs showing a maximum usable drain-source voltage of ∼70 V at 350°C on homoepitaxial diamond films. Homoepitaxial diamond films were grown on natural Ib insulating diamond crystal. A sandwich structure of 1 μm nominally undoped bottom layer/pulse-doped layer/120 nm nominally undoped top layer was grown on the diamond single crystal. The doping profile was obtained by inserting a boron rod into the plasma for a short period of 5 s. The peak doping level of the pulse was ∼10^{19} cm^{-3}, and the surface concentration of the top (Schottky) layer was below ∼10^{17} cm^{-3}. The ohmic contacts were formed on selectively grown $p+$ layers. The metallization for the ohmic and Schottky contacts was highly doped, sputtered $Si/WSi_2:N/Au$. The devices showed saturation and pinch-off characteristics up to 350°C. A maximum drain current of 5 mA/mm and a maximum transconductance of 0.22 mS/mm were reported at 350°C. The authors believe that steeper doping profiles (acceptor concentration of $>10^{20}$ cm^{-3}) with only a few monolayers in width are necessary to realize complete B activation leading to higher drain current and higher transconductance. For an optimized device structure, with gate length below 0.25 μm and full activation, more than 10 W/mm RF-power density is predicted.

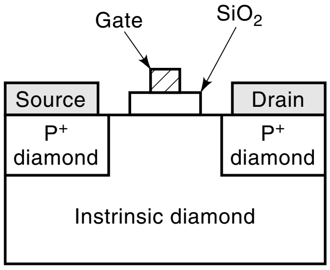

Figure 4. Schematic of a diamond p^+–i–p^+ transistor.

Das et al. (86) reported a p^{++}/undoped/p diamond rectifying structure. Subsequently, a transistor based on the p^+–i–p^+ structure was studied using numerical simulations (87). Figure 4 shows a schematic of a diamond p^+–i–p^+ transistor. Submicrometer gate p^+–i–p^+ diamond transistors with an SiO_2 gate insulator were studied by Miyata et al. (88) using 2-D device simulation. Accordingly, there are two important aspects in the present p^+–i–p^+ transistors. First, the holes are injected from p^+-diamond into i-diamond and transported by the space charge limited current (SCLC) mechanism in the i-region. Hence, the hole conduction is not influenced by the B acceptor level. The SCLC mechanism has been observed in rectifying contacts to diamond (89) as well as in metal-intrinsic, diamond-semiconducting diamond contacts (90). Second, an enormously large drain current exists in the accumulation mode, that is, when the gate is negatively biased. It has been shown through simulations that the transconductance of this device in the accumulation mode (∼70 mS/mm) is higher than that of a 6H–SiC MESFET in the depletion mode (88). Also, the calculated cut-off frequency of the diamond device for a gate length of 0.5 μm and the SiO_2 thickness of 500 Å was 31 GHz, which is better than that of a 6H–SiC MESFET.

COLD CATHODE DEVICES

Considering the technological importance of electron sources, there is a high level of activity in this area. Although devices requiring an electron source almost universally employ thermionic emitters, there is a great deal of effort directed toward the development of field emitters and planer emitters since thermionic emitters are inefficient with a limited life and contribute to major heat dissipation problems. Field emitters rely on emission from a pointed metal or semiconductor tip under the influence of a strong electric field. Significant progress has been reported in the achievement of high intensity electron sources. However, challenging problems pertaining to the uniformity and reliability of field emitters remain to be solved. Planar solid state emitters may provide an alternative to field emitters. Potential applications for these "solid-state" electron emitters include flat panel displays, vacuum microelectronic devices, and electron sources for microwave tubes. Semiconducting diamond structures are potentially capable of supporting both field-emitters and planar emitters.

Planar Emitters

Electron emission from planar semiconductor structures has been demonstrated by a number of research groups over the last thirty five years. For obtaining electron emission, various device structures, namely forward biased Schottky barriers and *p–n* junctions, reverse biased *p–n* junctions operating at avalanche, as well as npn structures have been employed. Generally, a small proportion of hot electrons, or electrons accelerated by an internal electric field established in a device, is available for emission. Those electrons reaching the surface with enough kinetic energy to be able to surmount the surface work function will be emitted into vacuum. The emission efficiency of early devices was low. In order to enhance emission, the solid surface is normally coated with about a monolayer of a material, such as Cs or CsO, in order to reduce the surface work function. Using an AlGaAs/GaAs doped barrier *n–i–p–i–n* structure with a delta doped *p* layer, Mishra and Jiang (91) reported an emitter efficiency of 1% with a cesiated surface. The *n–i–p–i–n* structure operating in the reach-through mode provides both an injecting as well as an accelerating region below the avalanche breakdown point. Figure 5 shows a schematic of electron emission from a forward biased *p–n* junction.

With narrow bandgap semiconductors, a substantial proportion of the carriers is transported by tunneling through the bandgap in the accelerating region. These tunneling carriers are unlikely to have enough kinetic energy to be emitted. The use of wider bandgap materials is expected to reduce the magnitude of the tunneling current. Therefore, wide bandgap materials such as SiC, GaN, GaP, and diamond are expected to yield higher efficiencies of emission. With the use of diamond with its demonstrated NEA properties, the need for Cs coating of the emitting surface may also be eliminated.

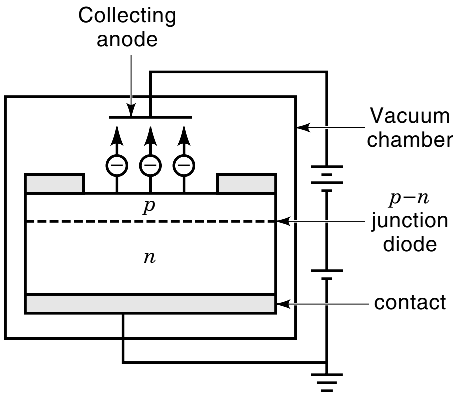

Figure 5. Schematic of the set-up used to obtain electron emission from a forward biased *p–n* junction.

Essentially, what is required is a mechanism by which electrons can be injected into the conduction band of *p*-type diamond and transported through the material that should have a thickness less than the diffusion length of the injected electrons (92). Geis et al. (93) have demonstrated the first *p–n* junction type cold cathode fabricated in naturally occurring semiconducting diamond and B doped homoepitaxial diamond films with (111) and (100) oriented substrates. They conducted a multiple implant of C ions with energies of 50, 106, and 170k eV with doses of 3.8×10^{16}, 3×10^{16} and 3.5×10^{16} cm^{-2}, respectively, into the *p*-type substrate maintained at a temperature of 320°C. A higher temperature implant provides a degree of in-situ annealing that maintains a degree of crystallinity. The associated stable damage contributes to a high *n*-type conductivity providing a *p–n* junction between the implanted layer and the substrate. Aluminum film of 1 μm in thickness was deposited on the entire implanted surface and patterned into 60×60 μm squares. The substrate was then etched to a depth of 1.1 μm, producing mesa structures with exposed junction edges. The substrates were then cleaned in an O_2 plasma and placed in a vacuum of the order of $\sim 1 \times 10^{-5}$ Torr and forward biased. Emitted electrons were collected by a positively biased anode. When the diodes were forward biased, electrons were injected from the implant-damaged *n*-type region to the *p*-type substrate. Those electrons injected within a diffusion length distance from the exposed junction edge were emitted into the vacuum. The emission may have been due entirely to diode injection and not due to NEA, as the orientation of the exposed surfaces do not exhibit NEA. Assuming electron-emission only from the perimeter of the device, the emission current density was estimated to be between 0.1 and 1 A/cm^2. This indicates that optimization of the diode design and processing may improve the emission densities from diamond *p–n* junction type cold cathodes.

Hot Electron Effect and Ballistic Transport

It has been postulated by Yoder (94) that semiconductors with large bandgaps, high dielectric strengths, and low optical phonon coupling to conduction band electrons may be capable of supporting electron energies well in excess of those limited by optical phonon energy. In II–VI compound semiconductors ZnS and ZnSe transistor structures designed to utilize ballistic transport, electrons were accelerated to energies up to 20 keV and injected into a vacuum without the application of an external electric field for the extraction of the electrons. Yoder (94) further postulates that in this device structure, wherein the electric field is parallel with a principal crystallographic axis and the semiconductor can support an electric field in excess of 5×10^5 V/cm, electrons can be accelerated to an energy sufficiently above the optical phonon energy such that optical phonon coupling and, hence, scattering becomes vanishingly small. Under such conditions, the effective mass of the electrons will approach that of electrons in vacuum, and electrons will gain energy well into keV range while still in the crystal. Since current densities of the order of 1×10^5 A/cm^2 can be produced in the semiconductor, high intensity cathodes are feasible with this technology. Owing to the crystalline structure of semiconducting materials, it is expected that these emitted electrons will be highly collimated, simplifying electron gun design. Recent measurements of electron energy distribution by Geis et al. (95) suggest ballistic transport in *n*-type diamond. This indicates the potential of diamond in the fabrication of high brightness cathodes. The high thermal conductivity of diamond is expected to be advantageous over Zn and ZnSe, which also exhibit ballistic transport.

Field Emitters

Using advanced electronic materials and present-day contact technology, metal/semiconductor junctions with vanishingly small barriers for electron injection can be produced; while in contrast, metal/vacuum barrier heights are typically on the order of 5 eV. Placing an electric field between two coplanar metal surfaces in a vacuum to initiate field emission requires, in theory, an impractically large voltage (96). To reproducibly surmount a 5 eV electron barrier, either high temperatures or a large applied electric field can be used to extract electrons. Typically, the implementation of the required electric fields is reduced in practice by utilizing a surface treatment to produce a surface dipole layer and/or the electric field enhancement created by sharp conducting points. Cesiation of semiconductor and metallic surfaces has been employed to engineer a reduction of the work function, but the properties of cesium which make it desirable, such as its electron affinity, also can result in a less than chemically robust surface (97). In contrast, sharpened tip structures exploit the reduced electric field penetration of conductors in order to create large field divergences at the tip. Empirical results for these structures have shown that the tip field E is inversely proportional to the tip radius of curvature (98). It is this enhanced field which promotes electron tunneling from the metal to the vacuum. Conversely, in material in which electric field penetration occurs, the penetration results in a reduction in field enhancement (99). Because of the highly developed nature of microfabrication methods and the robustness of metals, sharp points fabricated from conductors are the electron extraction method of choice. A comprehensive review of metal and silicon field emitting technology can be found in Brodie and Spindt (98). The attraction of using semiconducting materials as electron emitting material is the possibility of engineering a negative electron affinity surface (100). This would, in theory, substantially reduce the barrier between electrons in the semiconductor and the vacuum, thereby reducing the electric field required for electron extraction. Reduction of the required applied electric field is an important cost driver in device applications.

Field emission from semiconductors can generally occur through a greater variety of mechanisms than field emission from metals. Theoretical work (101–105) has investigated the possibility of field emission from the valence band, conduction band, and surface states. Under simplifying conditions, emission from each type of state has its own particular functional dependence on temperature and voltage. The functional form for the current-voltage characteristics for electron emission from a single conduction or valence band is similar to the Fowler-Nordheim equation for metals. For emission from the conduction band

$$I = I_c e^{-b_c/\beta V} \tag{1}$$

and for emission from the valence band

$$I = I_v V^2 e^{-b_v/\beta V} \tag{2}$$

where b is the field enhancement factor, and V is the applied voltage. The form of Eq. (2) is identical to the Fowler–Nordheim equation for metals. If the field penetration is negligible, then b is inversely proportional to the radius of curvature of the emitting site. I_c, b_c, I_v, b_v have similar meanings as in the metallic case and have a very slight dependence on the applied field through the Nordheim elliptic functions. A detailed analytical study of these dependencies has been reported by Modinos (104). In practice, I_c, b_c, I_v, b_v can be regarded as constants.

Field emission from surface states is highly model dependent, and experimental evidence is unclear. The history of the investigation of the origin of electrons in *p*-type germanium has interesting parallels to similar work reported for diamond. Results from germanium have been explained in terms of electron emission from the conduction band (106) surface states and the valence band (107). The valence band results were observed in high quality germanium (circa 1993), while in earlier published results, surface states and conduction band emission mechanisms were invoked. Materials quality issues were acknowledged by all the authors as a consideration in interpreting their results and so all of these explanations could be correct. Analogous questions raised in earlier investigations of *p*-type semiconductors also apply to diamond along with relevant work in the areas of field enhancement, field penetration, and electron drift distance.

Mechanisms. Diamond attracts interest as an electron emission material for several reasons. If it is considered as purely a field emission material candidate, carbon has one of the lowest sputtering yields of any metal or semiconductor and diamond has a work function of around 5 eV. In addition, the existence of negative electron affinity (NEA) has been reported for the hydrogen terminated (111) and (100) (108,109) surfaces, surfaces where the vacuum energy level is below the conduction band minimum. Exploitation of this phenomenon is dependent on the successful injection of electrons into the conduction band. As pointed out in Bandis and Pate (110), in *p*-type diamond, downward band bending at the surface is important in enhancing the near surface transport of electrons into the vacuum. Other materials besides hydrogen have also been used to terminate the diamond surface in an effort to investigate the effects of elemental monolayers on the electron affinity of diamond. Figure 6 shows a plot of the atomic electron affinity (111) versus reported electron affinity (112–116) of the material terminating the diamond surface. An important result of Fig. 6 is that any material that has an atomic electron affinity smaller than that of carbon appears to be a candidate for creating an NEA surface when monolayer coatings are applied to the diamond surface. Reports (117,118) indicate that a Cs terminated surface has an NEA. An unexamined alternative to Cs is B, which is estimated from Fig. 6 to have an NEA of around −0.6 eV. From Fig. 6, since B has a smaller atomic electron affinity than Cs, the value for its NEA is expected to be larger than Cs from this simple argument.

The original observation of NEA on the (111) diamond surface motivated an attempt to directly inject electrons into *p*-

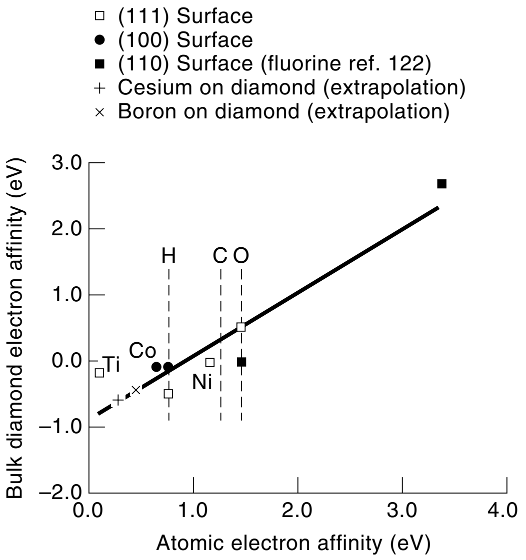

Figure 6. Plot of atomic electron affinity (eV) versus reported electron affinity of the material terminating the diamond surface.

type diamond (93). Subsequently, field emission from polycrystalline diamond was observed at tantalizing low fields (119). Since then, many observations have been made and possible mechanisms have been proposed, not all of them exploiting the NEA of diamond. Much work has been reported on the investigation of individual emission sites on B doped material (120–122). For p-type materials, it appears as though the most probable emission mechanism is the one indicated by Bandis and Pate (123). In carrying out simultaneous photoemission and field emission experiments, Bandis and Pate found that the measured electron energy distribution was composed of two parts, a photoemission part for which the electron origin was from the conduction band and a valence band component which remained after the UV excitation was removed. Fitting the energy distribution of the field emitted electrons to the theoretical form for emission from the valence band provided additional confirmation. Given that emission from the valence band would require a larger electric field than what was applied, Bandis and Pate concluded that electron tunneling from the valence band was facilitated by field enhancement and estimated a value for B of on the order of 100. Glesener and Morrish (124) also found that for p-type polycrystalline films, the emission current was independent of temperature. This additional finding is in accordance with the theoretical description for emission from the valence band. Information from current–voltage plots also indicated that the electron emission was from high B sites.

An example of where field enhancement issues are paramount is in the observed breakdown of the vacuum between two flat metal plates when a high voltage is applied. As examined in the review by Noer (96), in these situations field emission occurs at voltage factors of 100 to 1000 less than the ideal case at currents many orders of magnitude higher than the expected 10^{-18}A/cm^2. The current-voltage characteristics exhibited Fowler–Nordheim behavior, and the emission was typically found to have a surface distribution of tens of sites per cm^2. These sites were found to have measured field enhancement factors in the 100s. Of the possible models reviewed by Noer, two may have some practical relevance to diamond, the projection model and the effects of dielectric layers/inclusions. The projection model examines a mathematically solvable ideal in order to calculate B, the field enhancement factor, from first principles. In order to account for the observed βs in the 100s, the projection model requires that the projection height to diameter ratio to be approximately a factor of about 10. Several authors have attempted to observe such field emission structures in diamond without much success (125,126). This lack of observation would apparently constrain such features to nanometer sized dimensions. At the reported microampere emission currents, these dimensions would require large emission current densities.

The dielectric model postulates the existence of insulating inclusions or layers in which a conducting surface injects electrons into the conduction band of the insulator. The insulator supports a voltage drop which provides an additional impetus to the electrons. For p-type Si, owing to a strong correlation between increased surface charge and an increase in β, the results of Schroder et al. (99) indicate the importance of surface charging in screening the external electric field. Dielectric injection models require field penetration. At one extreme, there is B doped material where the lack of field penetration allows the possibility of field enhancement at the diamond/vacuum interface. At the other extreme, it has been hypothesized by several authors (95,121,126) that in insulating diamond, field penetration through the diamond would allow field enhancement at the metal/diamond interface and, thus, direct electron injection into the conduction band. Experimental work has been carried out on utilizing diamond powder with just this approach (95,127,128). A design difficulty with conduction band based electron emitters is a point considered by Bell (100) and further discussed by Bandis and Pate (110), regarding momentum conservation at the conduction band/vacuum boundary in diamond. Momentum conservation considerations at this interface impose directional constraints on the electron emission. In something as randomly oriented as a diamond powder coating, the direction of the emitted electrons may be difficult to control. This may explain the high gate currents reported in such devices (95).

A rarely discussed point with a practical impact on field emission models is the consideration of electron mobility on various proposed emission mechanisms, particularly electron injection models and models of heavily doped, poor quality diamond (129). The results for various low quality diamond samples report values for the electron drift distances ranging from 0.03 to 3 nm at field of about 0.5 V/μm (130). These results represent an upper limit on the electron drift distance because the combined electron/hole mobilities were measured. In a later paper with higher quality material, it was reported (131) that the drift distance saturated with respect to an increasing electric field at a value of 0.2 V/μm. It could be argued then that in field emitters based on low quality material, the diamond layer has to be sufficiently thin in order for electrons to traverse the film and enter the vacuum. Electron mobility considerations thus places a constraint on the thickness of the diamond layer in heavily doped or poor quality films.

Given the well known lack of a shallow donor in diamond, the argument for donor impurity bands as an electron source is a difficult one. The deeper the level of the donor, the smaller the hydrogenic component of the impurity wavefunction until at a given energy depth, a long range coulombic component is no longer an accurate representation of the wavefunction. Therefore, it is the range of the impurity wavefunction which is truncated with energy depth. Overcoming this trend with increasing trap-depth would require even higher impurity concentrations. This higher impurity concentration would again have a negative impact on carrier mobility.

Fabrication Methods. Processes to fashion sharpened diamond points are an attempt to impose regularity on the seemingly random distribution of emission sites displayed by polycrystalline films. Several methods have been employed to fabricate diamond tips. Well known silicon processing methods have been used to etch arrays of pyramidal voids into Si wafers. This forms the basis for a casting method for producing arrays of diamond pyramids. Under standard growth conditions, diamond coalesces to fill the etched pyramids (132,133). The sacrificial Si wafer is then etched away, exposing the pyramidal diamond emitters. The second method involves ion beam milling to shape blunt diamond surfaces into tips (134,136). Typically, Ar ions in the multi-keV range are used. The worthy goal of both fabrication methods is to eliminate chance in determining a field emission site. An unanswered question after such a procedure is the condition of the diamond surface and if this surface treatment is important to the operation of the device. The recent results of Huang et al. (137) show that the electronic structure of the diamond (100) surface is actually damaged under much more benign ion bombardment conditions (Ne^+ at 500 eV). It was reported that under such conditions, a defective layer approximately 2 nm thick was created. It appears as though such prepared surfaces are not diamond but, as Huang et al. (116) pointed out, neither are they graphite. A further potential drawback of ion bombardment is that it may increase the number of defect sites at which electron recombination can occur.

Alternative methods of fabricating arrays also exploit silicon processing technology. Several authors have used arrays of silicon needles as growth templates (138) and have demonstrated the growth of diamond particles at the needle tip. Growth of diamond on Si tips, while offering potentially superior materials properties, is perhaps at odds with the fundamental motivation for the use of silicon technology in vacuum microelectronics. Silicon is utilized in vacuum microelectronics not for its materials properties per se, but for its superior manufacturability and its ability to fabricate structures with extremely uniform electrical/mechanical parameters across a wide area. Current diamond growth methods are somewhat at odds with the process uniformities demanded by these silicon-based emitters.

Because of the tremendous but largely undocumented progress in carbonaceous emitters (139,140) in terms of turn-on voltage and areal uniformity over diamond, the remaining competitive area for diamond electron emitters is in SEDEs (surface engineering of diamond electron emitting materials) because of the possibility of binding NEA facilitating elements to the diamond surface. From an applied point of view, this is an area still worth pursuing because of the potential device advantages of a lowered extraction voltage that an NEA surface offers. Chemical surface treatments present a feasible research alternative to geometrical means of achieving uniform areal electron emission and potentially offer a wider process latitude. Further research is required to establish the influence on the properties of electron emission from diamond.

MISCELLANEOUS DEVICES

In addition to the major areas of interest in diamond electronic devices as discussed in the preceding sections, numerous other potential applications have been advanced. These applications exploit the wide bandgap, lattice stiffness, and thermal properties, which are superior to those of other electronic materials. Foremost among these ancillary applications is the use of diamond as energetic particle and electromagnetic radiation detectors, an application in which diamond appears to excel. Other device applications include piezoresistive strain sensors, thermistors, and chemical gas sensors. Pioneering work in these areas has been reviewed by Bazenov et al. (141) while current advances are covered by excellent reviews by Feldman (142), Pan (143), and Davidson and Kang (144).

CONCLUSION

Superior electronic properties of B doped diamond, including a wide bandgap of 5.45 eV, high saturated electron velocity, high breakdown field, low dielectric constant, and high hole mobility, suggest the possibility of high performance devices capable of operation at high frequency, power, temperature, and radiation levels. However, the absence of a truly heteroepitaxial diamond film and also the absence of a suitable *n*-type dopant will hinder diamond device development. Demonstrated devices at the present stage of development do not really take full advantage of the unique electronic properties of diamond, in particular, the high saturation velocity and low relative dielectric constant. It appears that devices based on new concepts will have to be developed in order to specifically take advantage of these unique properties of diamond.

BIBLIOGRAPHY

1. V. K. Bazhenov, I. M. Vikulin, and A. G. Gontar, *Sov. Phys. Semicond.,* **19**: 829, 1985.
2. K. Shenai, R. S. Scott, and B. J. Baliga, *IEEE Trans. Electron Devices,* **ED-36**: 1811, 1989.
3. G. S. Gildenblat, S. A. Grot, and A. Badzian, *Proc. IEEE,* **79**: 647, 1991.
4. M. W. Geis, *Proc. IEEE,* **79**: 669, 1991.
5. M. W. Shin, G. L. Bilbro, and R. J. Trew, High temperature operation of n-type 6H-SiC and p-type diamond MESFETs, in *Proc. IEEE/Cornell Conf. Advanced Concepts High Speed Semiconductor Devices Circuits,* Ithaca, N.Y. Aug. 1993, pp. 421–430.
6. R. W. Keyes, *Proc. IEEE,* **60**: 225, 1972.
7. E. O. Johnson, *RCA Rev.,* **26**: 163, 1965.
8. B. J. Baliga, *IEEE Electron Devices Lett.,* **10**: 455, 1989.
9. T. P. Chow and R. Tyagi, Wide bandgap compound semiconductors for superior high-voltage unipolar power devices, *IEEE Trans. Electron Devices,* **ED-41**: 1481–1483, 1994.
10. A. T. Collins and E. C. Lightowlers, in J. E. Field (ed.), *The properties of diamond,* San Diego: Academic Press, 1979, pp. 79–105.

11. G. H. Glover, *Solid-State Electronics,* **16**: 973, 1973.
12. K. Nishimura, K. Das, and J. T. Glass, *J. Appl. Phys.,* **69**: 3142–3148, 1991.
13. N. Fujimori, T. Imai, and A. Doi, *Vacuum,* **36**: 99, 1986.
14. M. W. Geis, in J. T. Glass, R. Messier, and N. Fujimori (eds.), Diamond, silicon carbide and related wide bandgap semiconductors, *Mat. Res. Soc. Symp. Proc.,* **162**: 15, 1990.
15. V. S. Vavilov et al., *Sov. Phys. Semicond.,* **4**: 6, 1970.
16. G. Braunstein and R. Kalish, *J. Appl. Phys.,* **54**: 2106, 1983.
17. J. F. Prins, *Phys. Rev. B,* **38**: 5576, 1988.
18. J. F. Prins, Modification, doping and devices in ion implanted diamond, in J. E. Field (ed.), *The properties of natural and synthetic diamond,* New York: Academic Pressss, 1992.
19. R. Kalish, Ion implantation and diffusion, in G. Davies (ed.), *Properties and growth of diamond,* Stevenage, UK: IEE/INSPEC, 1994.
20. K. Das, Electronic applications of diamond films and coatings, in R. F. Davis (ed.), *Diamond films and coatings,* Park Ridge, NJ: Noyes Publications, 1993.
21. B. A. Fox et al., Electrical properties of diamond for device applications, *MRS Symp. Proc.,* **416**: pp. 319–330, 1996.
22. J. C. Angus and A. T. Collins, Electronic era elusive, *Nature,* **370**: 601, 1994.
23. V. S. Vavilov, *Radiation Eff.,* **37**: 229, 1978.
24. G. G. Fountain et al., IGFET fabrication on homoepitaxial diamond using in situ boron and lithium doping, in A. J. Purdes et al. (eds.), Diamond materials, *Electrochem. Soc. Proc.,* **91–8**: 523, 1991.
25. K. Okumura, J. Mort, and M. Machonkin, *Appl. Phys. Lett.,* **57**: 1907, 1990.
26. C. P. Beetz Jr., B. A. Lincoln, and D. R. Winn, in A. Feldman, and S. Holly (eds.), *Diamond optics III,* SPIE, **1325**: 241, 1990.
27. J. F. Prins, Ion-implanted n-type diamond: electrical evidence, *Diamond Related Mater.,* **4**: 580–585, 1995.
28. G. Popovici et al., Properties of diffused diamond films with n-type conductivity, *Diamond Related Mater.,* **4**: 877–881, 1995.
29. C. P. Beetz Jr. and B. Lincoln, in R. Messier et al. (eds.), *Proc. 2nd Int. Conf. New Diamond Sci. Tech., Mater. Res. Soc.,* Pittsburgh, 1991, p. 975.
30. M. N. Efremow et al., *J. Vac. Sci. Technol.,* **B3**: 416, 1991.
31. K. Kobashi et al., in R. Messier et al. (eds.), *Proc. 2nd Int. Conf. New Diamond Sci. Tech., Mater. Res. Soc.,* Pittsburgh, 1991, p. 975.
32. H. Kawarada et al., Characterization of hydrogen-terminated CVD diamond surfaces and their contact properties, *Diamond Related Mater.,* **3**: 961–965, 1994.
33. N. R. Parikh et al., Diamond Optics, *SPIE Proc.,* **969**: 95, 1988.
34. M. I. Landstrass and K. V. Ravi, *Appl. Phys. Lett.,* **55**: 1391, 1989.
35. S. Albin and L. Watkins, *IEEE Electron Devices Lett.,* **11**: 159, 1990.
36. S. A. Grot et al., *IEEE Electron Devices Lett.,* **11**: 100, 1990.
37. Y. Mori, H. Kawarada, and A. Hiraki, *Appl. Phys. Lett.,* **58**: 940, 1991.
38. J. Shirafuji and T. Sugino, Electrical properties of diamond surfaces, *Diamond Related Mater.,* **5**: 706–713, 1996.
39. W. Kern and D. A. Puotinen, *RCA Rev.,* **31**: 187, 1970.
40. J. F. Prins, *Appl. Phys. Lett.,* **41**: 950, 1982.
41. M. W. Geis et al., *IEEE Electron Devices Lett.,* **8**: 341, 1987.
42. K. L. Moazed, *Met. Trans. A.,* **23**: 1999, 1992.
43. T. Tachibana, B. E. Williams, and J. T. Glass, *Phys. Rev. B,* **45**: 11968, 1992.
44. T. Tachibana, B. E. Williams, and J. T. Glass, *Phys. Rev. B,* **45**: 11975, 1992.
45. F. Fang et al., *IEEE Trans. Electron Devices,* **36**: 1783, 1989.
46. C. B. Childs, G. S. Sandhu, and W. K. Chu, presented at the 4th SDIO/IST-ONR *Diamond Tech. Initiative Symp.,* Crystal City, VA, July 1989.
47. G. S. Sandhu, Ph.D. Thesis, University of North Carolina, Chapel Hill, 1989.
48. J. F. Prins, *J. Phys. D. Appl. Phys.,* **22**: 1562, 1989.
49. C. A. Hewett et al., in R. Messier et al. (eds.), *Proc. 2nd Int. Conf. New Diamond Sci. Tech., Mater. Res. Soc.,* Pittsburgh, 1991, p. 1107.
50. V. Venkatesan, D. M. Malta, and K. Das, Evaluation of ohmic contacts formed by B^+ implantation and Ti-Au metallization on diamond, *J. Appl. Phys.,* **74**: 1179, 1993.
51. M. Werner et al., Electrical characterization of Al/Si ohmic contacts to heavily boron doped polycrystalline diamond films, *J. Appl. Phys.,* **79** (5): 2535–2541, 1996.
52. K. Das, V. Venkatesan, and T. P. Humphreys, Ohmic contacts on diamond by B ion implantation and TiC-Au and $TaSi_2$-Au metallization, *J. Appl. Phys.,* **76** (4): 2208, 1994.
53. M. Geis, J. Gregory, and B. Pate, *IEEE Trans. Electron Devices,* **38**: 619, 1991.
54. E. C. Lightowlers and A. T. Collins, *J. Phys. D: Appl. Phys.,* **9**: 951, 1976.
55. H. Shiomi, Y. Nishibayashi, and N. Fujimori, in R. Messier et al. (eds.), *Proc. 2nd Int. Conf. New Diamond Sci. Tech., Mater. Res. Soc.,* Pittsburgh, 1991, p. 975.
56. K. Miyata, D. Dreifus, and K. Kobashi, *Appl. Phys. Lett.,* **60**: 480, 1992.
57. V. Venkatesan et al., Effect of thin interfacial SiO_2 films on metal contacts to boron doped diamond films, *J. Electrochem. Soc.,* **139**: 1445, 1992.
58. K. Das et al., presented at the Third International Symposium on Diamond Materials, *183rd Meet. Electrochem. Soc., Inc.,* Honolulu, HI, May 16–21, 1993.
59. T. P. Humphreys et al., *Jpn. J. Appl. Phys.* **30**: L1409, 1991.
60. P. K. Baumann et al., Epitaxial Cu contacts on semiconducting diamond, *Diamond Related Mater.,* **3**: 883–886, 1994.
61. S. R. Sahaida and D. G. Thompson, in T. D. Moustakos, J. I. Pankove, and Y. Hamakawa (eds.), Wide Bandgap Semiconductors, *Mater. Res. Soc. Symp. Proc.,* **242**: 1992, p. 151.
62. V. Venkatesan, D. G. Thompson, and K. Das, High temperature rectifying contacts on diamond using doped silicon, in C. L. Renschler et al. (eds.), Novel forms of Carbon, *Mater. Res. Soc. Symp. Proc.,* **270**: 1992, p. 419.
63. C. A. Mead and T. C. McGill, *Phys. Lett.,* **58A**: 249, 1976.
64. V. Venkatesan et al., The effect of back contact impedance on frequency dependence of capacitance-voltage measurements on metal/diamond diodes, *Appl. Phys. Lett.,* **63**: 1065, 1993.
65. F. J. Himpsel, P. Heimann, and D. E. Eastman, *Solid State Comm.,* **36**: 631, 1980.
66. M. C. Hicks et al., *J. Appl. Phys.,* **65**: 2139, 1989.
67. J. M. Shannon, Reducing the effective height of a Schottky barrier using low-energy ion implantation, *App. Phys. Lett.,* **24** (8): 369–371, 1974.
68. M. Teklu and K. Das, Barrier modification in Au/IIb semiconducting diamond ohmic contacts, in D. L. Dreifus et al. (eds.), Diamond for electronic applications, *Mater. Res. Soc. Symp. Proc.,* **416**: Pittsburgh, 1966, pp. 151–155.
69. H. A. Wynands, M. L. Hartsell, and B. A. Fox, Characterization of MS, MiS, and MOS contacts to type IIb diamond by capacitance-voltage and current-voltage, in C. Carter et al. (eds.), Dia-

mond, SiC and nitride wide bandgap semiconductors, *Mater. Res. Soc. Symp. Proc.,* **339**: 1994, pp. 235–240.

70. K. Nishimura et al., Fabrication of field effect transistors made of polycrystalline diamond films, in J. P. Dismukes et al. (eds.), *Diamond Materials,* Pennington. NJ: The Electrochem. Soc., 1993, p. 940–946.
71. A. J. Tessmer, L. S. Plano, and D. L. Dreifus, *IEEE Electron. Devices. Lett.,* **14**: 66, 1993.
72. D. L. Dreifus et al., High temperature operation of diamond field-effect transistors, *Trans. 2nd Int. High Temperature Electron. Conf.,* **1**: Charlotte, NC, June 5–10, 1994, pp. VI-29–VI-34.
73. J. R. Zeidler, C. A. Hewett, and R. Nguyen, Material aspects of diamond-based electronic devices, in C. Carter et al. (eds.), Diamond, SiC and nitride wide bandgap semiconductors, *Mater. Res. Soc. Symp. Proc.,* **339**: Pittsburgh, 1994, 109–120.
74. S. A. Grot, G. S. Gildenblat, and A. R. Badzian, *IEEE Electron Devices Lett.,* **13**: 462, 1992.
75. M. A. Plano, M. D. Moyer, and M. M. Moreno, CVD diamond, presented at the 2nd Int. High Temperature Electron. Conf., Charlotte, NC, 1994, p. VI-23.
76. W. Tsai et al., *IEEE Electron Devices Lett.,* **12**: 157, 1991.
77. M. W. Geis, N. N. Efremow, and D. D. Rathman, *J. Vac. Sci. Technol. A,* **6**: 1853, 1988.
78. H. Kawarada, M. Aoki, and M. Ito, Enhancement-mode metal-semiconductor field-effect transistors using homoepitaxial diamonds, *Appl. Phys. Lett.,* **65** (12): 1563–1565, 1994.
79. J. S. Holmes, A. J. Tessmer, and D. L. Dreifus, High temperature operation of diamond digital logic structures, *Trans. 2nd Int. High Temperature Electron. Conf.,* **1**: Charlotte, NC, June 5–10, 1994, pp. VI-35–VI-40.
80. A. J. Tessmer, K. Das, and D. Dreifus, *Diamond and Related Mater.,* **1**: 89, 1992.
81. D. L. Dreifus et al., Diamond field-effect transistors, in C. Carter et al. (eds.), Diamond, SiC and nitride wide bandgap semiconductors, *Mater. Res. Symp. Proc.,* **339**: 1994, pp. 109–120.
82. K. Nishimura et al., Metal/intrinsic semiconductor/semiconductor field effect transistor fabricated from polycrystalline diamond films, *J. Appl. Phys.,* **76** (12): 8142–8145, 1994.
83. T. Kobayashi et al., Analytical studies on multiple delta doping in diamond thin films for efficient hole excitation and conductivity enhancement, *J. Appl. Phys.,* **76** (3): 1977–1979, 1994.
84. H. Shiomi et al., Pulse-doped diamond p-channel metal semiconductor field-effect transistor, *IEEE Elec. Devices Lett.,* **16** (1): 36–38, 1995.
85. A. Vescan et al., High-temperature, high-voltage operation of pulse-doped diamond MESFET, *IEEE Elec. Devices Lett.,* **18** (5): 222–224, 1997.
86. K. Das, C. T. Kao, and L. S. Plano, A novel p++/undoped/p diamond rectifying structure, in M. Yoshikawa et al. (eds.), *2nd Int. Conf. App. Diamond Films and Related Mater.,* Tokyo, 1993, pp. 335–340.
87. B. Buchard et al., 2D-simulation of diamond based electronic devices. In S. Saito et al. (eds.), *Advances in Diamond Science and Technology,* Tokyo, 1994, pp. 721–724.
88. K. Miyata, K. Nishimura, and K. Kobashi, Device simulation of submicrometer gate p^+-i-p^+ diamond transistors, *IEEE Trans. Electron Devices,* **42**: 2010–2014, 1995.
89. V. Venkatesan, J. A. von Windheim, and K. Das, Deep-level effects on forward characteristics of rectifying contacts on semiconducting diamond, *IEEE Trans. Electron Devices,* **40**: 1556, 1993.
90. K. Miyata and D. L. Dreifus, Metal/intrinsic diamond/semiconducting diamond junction diodes fabricated from polycrystalline diamond films, *J. Appl. Phys.,* **73**: 4448–4456, 1993.
91. U. K. Mishra and W. N. Jiang, Planar cold cathodes, presented at the *High Speed Devices Conf.,* Cornell University, Ithaca, NY, Aug. 1993.
92. N. M. Miskovsky et al., Theory of electron emission and transport properties of diamond, in D. L. Dreifus et al. (eds.), Diamond for electronic applications, *Mater. Res. Soc. Symp. Proc.,* **416**, Pittsburgh, 1996.
93. M. W. Geis et al., Diamond cold cathode, *IEEE Trans. Electron Devices,* **12**: 456–459, 1991
94. M. N. Yoder, Wide bandgap semiconductor materials and devices, *IEEE Trans. Electron Devices,* **43**: 1633–1636, 1996.
95. M. W. Geis, J. C. Twitchell, and T. M. Lyszczarz, Diamond emitters fabrication and theory, *J. Vac. Sci. Technol.,* **B14**: 2060–2069, 1996.
96. R. J. Noer, Electron field emission from broad-area electrodes, *Appl. Phys. A,* **28**: 1–24, 1982.
97. A. M. E. Hoeberechts and G. G. P. van Gorkom, Design, technology and behavior of a silicon avalanche cathode, *J. Vac. Sci. Technol.,* **B4**: 105–107, 1986.
98. I. Brodie and C. A. Spindt, Vacuum Microelectronics, in P. W. Hawkes (ed.), *Advances in Electronics and Electron Physics,* **83**: Boston: Academic Press, 1992, pp. 1–106.
99. D. K. Schroder et al., The semiconductor field-emission photocathode, *IEEE Trans. Electron Devices,* **ED-21**: 785–798, 1974.
100. R. L. Bell, *Negative Electron Affinity Devices,* Clarendon: Oxford, 1973.
101. R. Stratton, Theory of field emission from semiconductors, *Phys. Rev.,* **125**: 67–82, 1961.
102. S. G. Christov, Unified theory of thermionic and field emission from semiconductors, *Phys. Stat. Sol.,* **21**: 159–173, 1967.
103. L. M. Baskin, O. I. Lvov, and G. N. Fursey, General features of field emission from semiconductors, *Phys. Stat. Sol.,* **47b**: 49–62, 1971.
104. A. Modinos, *Field, Thermionic, and Secondary Electron Emission Spectroscopy,* New York: Plenum, 1984.
105. Z. H. Huang et al., Calculation of electron field emission from diamond surfaces, *J. Vac. Sci. Technol.,* **B13**: 526–530, 1995.
106. J. R. Arthur, Photosensitive field emission from p-type germanium, *Phys. Rev.,* **36**: 3221–3227, 1965.
107. V. D. Kalganov, N. V. Mileshkina, and S. A. Sapronov, Energy distribution of field-emitted electrons from p-type germanium, *Vacuum,* **46**: 559–561, 1995.
108. F. J. Himpsel et al., Quantum photoyield of diamond (111)-A stable negative-affinity surface, *Phys. Rev.,* **B20**: 624–627, 1979.
109. J. van der Weide et al., Negative-electron-affinity effects on the diamond (100) surface, *Phys. Rev. B,* **50**: 5803–5806, 1994.
110. C. Bandis and B. B. Pate, Photoelectric emission from negative-electron-affinity diamond (111) surfaces: exciton breakup versus conduction-band emission, *Phys. Rev. B2,* **52**: 12056–12071, 1995.
111. R. C. Weast (ed.), *CRC Handbook of Chemistry and Physics,* 66th ed., Boca Raton: CRC Press, 1985, p. E-62.
112. N. Eimori et al., Electron affinity of single-crystalline chemical vapor deposited diamond studied by ultraviolet synchrotron radiation, *Jpn. J. Appl. Phys.,* **33** (1): 6312–6315, 1994.
113. J. van der Weide and R. J. Nemanich, Schottky barrier height and negative electron affinity of titanium on (111) diamond, *J. Vac. Sci. Technol.,* **B10**: 1940–1943, 1992.
114. J. van der Weide and R. J. Nemanich, Influence of interfacial hydrogen and oxygen on the Schottky barrier height of nickel an (111) and (100) diamond surfaces, *Phys. Rev. B1,* **49**: 13629–13637, 1994.
115. P. K. Baumann and R. J. Nemanich, Negative electron affinity effects and the schottky barrier height measurements of cobalt

on diamond (100) surfaces, in A. Feldman (ed.), *Proc. 3rd Int. Appl. Diamond Conf.,* NIST special publication **885**: 1995, pp. 41–44.

116. C. A. Fox et al., Cesiation of fluorinated diamond and diamond-like carbon surfaces, submitted to *Appl. Phys. Lett.,* 1997.
117. W. E. Pickett, Negative electron affinity and low work function surface: Cesium on oxygenated diamond (100), *Phys. Rev. Lett.,* **73**: 1664–1667, 1994.
118. C. A. Fox et al., Photoelectron emission from the cesiated diamond (110) surface, in D. Dreifus et al. (eds.), *MRS Symp. Proc.,* **416**, Pittsburgh: Materials Research Soc., 1996.
119. C. Wang et al., Cold field-emission from CVD diamond films observed in emission electron microscopy, *Electron. Lett.,* **27**: 1459–1461, 1991.
120. N. S. Xu, R. V. Latham, and Y. Tzeng, Field-dependence of the area density of 'cold' electron emission sites on broad area CVD diamond films, *Electron. Lett.,* **29**: 1596–1597, 1993.
121. N. S. Xu, Y. Tzeng, and R. V. Latham, A diagnostic study of the field emission characteristics of individual micro-emitters in CVD diamond films, *J. Phys. D: Appl. Phys.,* **27**: 1988–1991, 1994.
122. M. W. Geis et al., Electron field emission from diamond and other carbon materials after H_2, O_2, and Cs treatment, *Appl. Phys. Lett.,* **67**: 1328–1330, 1995.
123. C. Bandis and B. B. Pate, Simultaneous field emission and photoemission from diamond, *Appl. Phys. Lett.,* **69**: 366–368, 1996.
124. J. W. Glesener and A. A. Morrish, Investigation of the temperature dependence of the field emission current of polycrystalline diamond films, *Appl. Phys. Lett.,* **69**: 785–787, 1996.
125. N. Pupeter et al., Field emission measurements with micron resolution on chemical-vapor-deposited poly crystalline diamond films, *J. Vac. Sci. Technol.,* **B14**: 2056–2059, 1996.
126. A. A. Talin et al., The relationship between the spatially resolved field emission characteristics and the Raman spectra of a nanocrystalline diamond cold cathode, *Appl. Phys. Lett.,* **69**: 3842–3844, 1996.
127. J. W. Glesener and A. A. Morrish, *Electron field emission,* U.S. Patent No. 5,619,093, 1997.
128. R. Schlesser et al., Energy distribution of field emitted electrons from diamond coated moly bdenum tips, *Appl. Phys. Lett.,* **70**: 1596–1598, 1997.
129. W. Zhu et al., Electron field emission from chemical vapor deposited diamond, *J. Vac. Sci. Technol.,* **B14**: 2011–2019, 1996.
130. L. S. Pan et al., Electrical transport properties of undoped CVD diamond films, *Science,* **255**: 830–833, 1992.
131. M. A. Plano et al., Polycrystalline diamond films with high electrical mobility, *Science,* **260**: 1310–1312, 1993.
132. K. Okano, K. Hoshina, and M. Iida, Fabrication of a diamond field emitter array, *Appl. Phys. Lett.,* **64**: 2742–2744, 1994.
133. J. L. Davidson, in A. Feldman (ed.), *Proc. 3rd Int. Appl. Diamond Conf.,* NSIT special publication **885**: 1995, pp. 41–44.
134. T. Asano, Y. Oobuchi, and S. Katsurmata, Field emission from ion-milled diamond films on Si, *J. Vac. Sci. Technol.,* **B13**: 431–434, 1995.
135. C. Nutzenadel et al., Electron field emission from diamond tips prepared by ion sputtering, *Appl. Phys. Lett.,* **69**: 2662–2664, 1996.
136. V. Raiko et al., Field emission from CVD diamond-coated silicon emitters, *Thin Solid Films,* **290–291**: 190–195, 1996.
137. L. J. Huang et al., Synchrotron radiation x-ray absorption of ion bombardment induced defects on diamond (100), *J. Appl. Phys.,* **76**: 7483–7486, 1994.
138. E. I. Givargizov et al., Cold emission from the single-crystalline microparticle of diamond on a Si tip, *J. Vac. Sci. Technol.,* **B14**: 2030–2033, 1995.
139. N. Kumar, H. Schmidt, and C. Xie, Diamond-based field emission flat panel displays, *Solid State Technol.,* **38**: 71–74, 1995.
140. J. Jaskie, The status of diamond-based field emission displays, presented at the *Int. Conf. Met. Coatings and Thin Films,* San Diego, 1997.
141. V. K. Bazenov, I. M. Vikulin, and A. G. Duntar, Synthetic diamonds in electronics, *Sov. Phys. Semicond.,* **19**: 829–841, 1985.
142. A. Feldman (ed.), Proc. 3rd Int. Appl. Diamond Conf., *NIST Special Publication,* 1995, p. 885.
143. L. S. Pan, Diamond sensors and vacuum microelectronics, in D. Dreifus et al. (eds.), *MRS Symp. Proc.,* **416**: Pittsburgh: Materials Research Society, 1996, pp. 407–418.
144. J. L. Davidson and W. P. Kang, Examples of diamond sensing applications, in D. Dreifus et al. (eds.), *MRS Symp. Proc.,* **416**, Pittsburgh: Materials Research Society, 1996, pp. 407–418.

V. Venkatesan
Motorola Inc.
J. W. Glesener
Naval Research Laboratory, Code 5674
K. Das
Tuskegee University

DIELECTRIC DEFECT LOCATION. See Partial discharges.

DIELECTRIC INSULATION. See Capacitor insulation.

DIELECTRIC ISOLATION. See Isolation technology.

DIELECTRIC LIQUIDS, CONDUCTION AND BREAKDOWN. See Conduction and breakdown in dielectric liquids.